

# The influence of quenching rate on the magnetic properties of microcrystalline alloys $\text{Co}_{80}\text{Zr}_{20-x}\text{B}_x$

G. Stroink, Z. M. Stadnik, G. Viau, and R. A. Dunlap

Department of Physics, Dalhousie University, Halifax, Nova Scotia B3H 3J5, Canada

Magnetic properties of melt-spun  $\text{Co}_{80}\text{Zr}_{20-x}\text{B}_x$  microcrystalline alloys ( $0 < x < 8$ ) depend crucially on the quench rate. The optimized values of  $H_c = 2.68$  kOe and  $(BH)_{\text{max}} = 2.10$  MG Oe were obtained for  $\text{Co}_{80}\text{Zr}_{16}\text{B}_4$  melt-spun with the substrate surface velocity of 48 m/s. A new crystalline phase of  $\text{Co}_5\text{Zr}$  was observed.

## I. INTRODUCTION

Rapidly quenched  $\text{Co}_{80}\text{Zr}_{20-x}\text{B}_x$  alloys were studied first by Ghemawat, McHenry, and O'Handley.<sup>1</sup> It was found that samples melt-spun with a substrate surface velocity of  $v_s = 26$  m/s were amorphous for  $8 < x < 20$  and crystalline for  $x < 8$ . An increase of magnetic moment per Co atom with  $x$  was interpreted within Friedel's virtual bound state model and by invoking  $p-d$  and  $d-d$  hybridization between B and Zr, and Co and Zr. In a subsequent paper, Ghemawat *et al.*<sup>2</sup> studied melt-spun samples produced with  $v_s = 27$  m/s and suggested the possibility of using crystalline alloys with  $x = 2$  and 4 as hard magnets. The energy product  $(BH)_{\text{max}}$  values of 5.5 MG Oe were reported<sup>2</sup> for these compositions. The largest value of the coercive force  $H_c = 3.3$  kOe was reported for the  $x = 4$  composition.<sup>2</sup> In order to provide a consistent comparison with the present results, we have reanalyzed the original data of Ref. 2 for the  $\text{Co}_{80}\text{Zr}_{16}\text{B}_4$  sample and have obtained  $H_c = 3.3$  kOe,  $M_r = 4.7$  kG, and  $(BH)_{\text{max}} = 3.5$  MG Oe. Ghemawat and co-workers<sup>1,2</sup> did not identify an intermetallic phase (nor phases) responsible for the magnetic properties of the investigated alloys.

It is now well established that the magnetic properties of melt-spun hard magnets are in general sensitive to the quench rate.<sup>3</sup> In previous studies<sup>1,2</sup> on the  $\text{Co}_{80}\text{Zr}_{20-x}\text{B}_x$  series the samples were produced for only one value of  $v_s$ . The purpose of this paper is to study magnetic parameters of this series as a function of  $v_s$  in order to determine the composition and the value of  $v_s$  giving the optimum hard magnetic parameters. Furthermore, an attempt is made to identify the intermetallic phase (phases) which gives rise to the hard magnetic properties of the  $\text{Co}_{80}\text{Zr}_{20-x}\text{B}_x$  series.

## II. EXPERIMENT

Samples of the composition  $\text{Co}_{80}\text{Zr}_{20-x}\text{B}_x$  ( $x = 0, 1, 2, 4, 6,$  and  $8$ ) were produced by induction melting high-purity elemental constituents under argon. Each ingot was melt spun in a helium atmosphere by ejecting molten alloy through an orifice (0.61 or 0.81 mm in diameter) in a quartz tube onto the surface of a rotating copper wheel, resulting in ribbons typically 2 mm wide and 30  $\mu\text{m}$  thick.

X-ray diffraction measurements were performed using a Siemens D500 diffractometer with  $\text{CuK}\alpha$  radiation. Room-temperature magnetization measurements were conducted using a vibrating sample magnetometer in fields up to 9 kOe.

## III. RESULTS AND DISCUSSION

The strong influence of boron concentration on the magnetic properties of the  $\text{Co}_{80}\text{Zr}_{20-x}\text{B}_x$  series is demonstrated in Fig. 1. It is seen that a substitution of only 5% of the Zr by B atoms leads to a significant increase in the magnetization measured at 9 kOe. For the samples studied here the magnetization shows a general increase with  $x$  (Table I), which is in agreement with the results of previous studies.<sup>1,2</sup> Also, the magnetic moment at 4.2 K of  $0.70 \mu_B$  per Co atom for  $\text{Co}_{80}\text{Zr}_{20}$  derived from the magnetization measured at 9 kOe,  $M_9$  (Table I), agrees with the value extrapolated from the experimental data of Ref. 1.

Figure 2 shows a dramatic influence of the quench rate on the magnetic parameters of the  $\text{Co}_{80}\text{Zr}_{16}\text{B}_4$  alloy. The ingot sample cannot be saturated in the field of 9 kOe and has negligibly small  $H_c$  and  $M_r$  [Fig. 2(a)]. The sample melt-spun with  $v_s = 48$  m/s [Fig. 2(b)] is almost saturated in the field of 9 kOe and exhibits relatively large  $H_c$  and  $M_r$ . Further increase of the quench rate leads to the disappearance of  $H_c$  and  $M_r$  [Fig. 2(c)]. Figure 2 also illustrates the general trend observed for this series of an increase in saturation magnetization with increasing quench rate.

The room-temperature magnetic parameters of the  $\text{Co}_{80}\text{Zr}_{20-x}\text{B}_x$  series were determined for a wide range of  $v_s$ ,

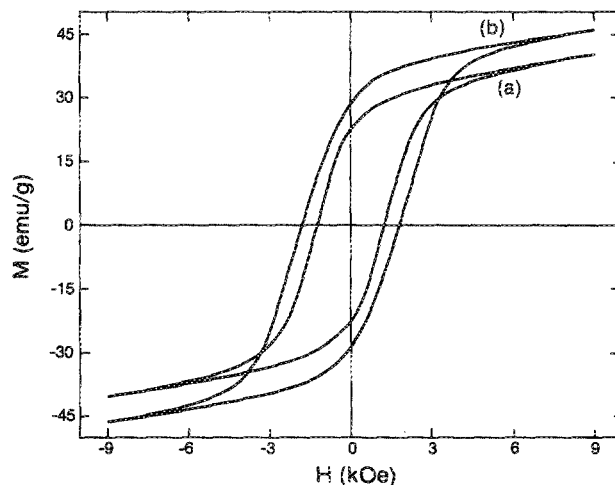


FIG. 1. Room-temperature hysteresis curves for melt-spun ( $v_s = 60$  m/s) (a)  $\text{Co}_{80}\text{Zr}_{20}$  and (b)  $\text{Co}_{80}\text{Zr}_{16}\text{B}_4$ .

TABLE I. Composition  $x$ , calculated density  $\rho$ , substrate surface velocity  $v_s$ , room-temperature magnetization measured in the field of 9 kOe,  $M_9$ , ratio of remanence magnetization  $M_r$  and  $M_9$ , coercive force  $H_c$ , and energy product  $(BH)_{\max}$  for  $\text{Co}_{80}\text{Zr}_{20-x}\text{B}_x$  alloys.

$x$	$\rho$ (g/cm <sup>3</sup> )	$v_s$ (m/s)	$M_9$ (emu/g)	$M_r/M_9$	$H_c$ (kOe)	$(BH)_{\max}$ (MG Oe)
0	8.42	40 <sup>a</sup>	41.1	0.59	1.37	0.70
		60 <sup>a</sup>	40.0	0.91	1.24	0.91
		60 <sup>a</sup>	47.9 <sup>b</sup>	0.61 <sup>b</sup>	1.34 <sup>b</sup>	1.34 <sup>b</sup>
1	8.38	60 <sup>a</sup>	45.8	0.62	1.81	1.00
2	8.34	60 <sup>a</sup>	51.8	0.41	1.33	0.51
4	8.25	... <sup>c</sup>	46.5	0.06	0.15	~0.0
		30 <sup>a</sup>	58.0	0.69	0.84	1.24
		36 <sup>a</sup>	56.7	0.71	1.26	1.24
		42 <sup>a</sup>	53.7	0.71	2.25	1.89
		48 <sup>a</sup>	60.0	0.41	0.59	0.31
		60 <sup>a</sup>	68.1	0.10	0.09	~0.0
		69 <sup>a</sup>	74.2	~0.0	~0.0	~0.0
		36 <sup>d</sup>	56.3	0.54	1.76	0.96
		42 <sup>d</sup>	53.8	0.53	1.57	0.83
48 <sup>d</sup>	57.6	0.70	2.68	2.10		
54 <sup>d</sup>	62.7	0.51	1.92	1.10		
69 <sup>d</sup>	74.0	~0.0	~0.0	~0.0		
6	8.17	... <sup>c</sup>	60.1	0.10	0.17	~0.0
		42 <sup>a</sup>	72.6	~0.0	0.0	~0.0
		60 <sup>a</sup>	84.8	~0.0	~0.0	~0.0
8	8.09	... <sup>c</sup>	67.6	0.10	0.10	~0.0
		42 <sup>a</sup>	80.0	0.0	0.0	0.0
		60 <sup>a</sup>	78.1	0.0	0.0	0.0

<sup>a</sup> Orifice diameter of 0.61 mm.

<sup>b</sup> Measured at 4.2 K.

<sup>c</sup> Ingot.

<sup>d</sup> Orifice diameter of 0.8 mm.

values. Some of the data are presented in Table I. In determining the energy product  $(BH)_{\max}$  an assumption was made that an alloy density is a linear combination of the elemental densities in proportion to their concentrations.<sup>4</sup> This assumption leads to an estimated inaccuracy in determining  $(BH)_{\max}$  of 5%.

For a given quench rate,  $M_9$  increases with boron concentration. For a given concentration,  $M_9$  generally increases with increasing quench rate (Table I). Changes of other magnetic parameters with the quench rate and composition are more complex. The data in Table I show that  $M_r/M_9$ ,  $H_c$ , and  $(BH)_{\max}$  are more strongly dependent on composition and quench rate than  $M_9$ . A similar observation was made for  $H_c$  changes in Nd-Co-B magnets.<sup>5</sup> As is seen from Table I, the optimum values of remanence, coercive force, and energy product are obtained for the  $\text{Co}_{80}\text{Zr}_{16}\text{B}_4$  composition with a substrate surface velocity of 48 m/s.

The optimum values of  $H_c = 2.68$  kOe and  $(BH)_{\max} = 2.10$  MG Oe obtained in this work are somewhat smaller than the values of  $H_c = 3.3$  kOe and  $(BH)_{\max} = 3.5$  MG Oe obtained from the data of Ref. 2. This, along with an inspection of Table I, clearly shows the sensitivity of the hysteretic properties of these alloys to minor changes in composition

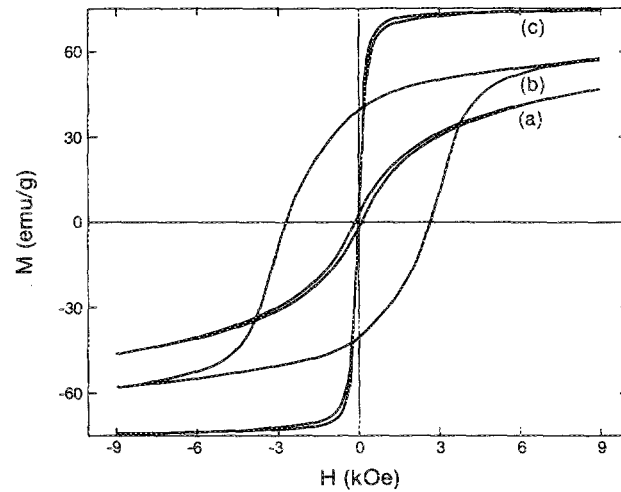


FIG. 2. Room-temperature hysteresis curves for (a)  $\text{Co}_{80}\text{Zr}_{16}\text{B}_4$  ingot and samples melt spun from it at (b)  $v_s = 48$  m/s and (c)  $v_s = 69$  m/s.

and processing conditions. While the measured hard magnetic properties of these materials do not compare with present rare-earth-containing magnets (Co-Sm and Nd-Fe-B), they do compare favorably with many ferrite and Alnico-type magnets<sup>6</sup> presently in use. The viability of these materials for particular commercial applications would require a detailed analysis of processing conditions to optimize the magnetic properties for these applications.

Figure 3 shows x-ray diffraction patterns of the  $\text{Co}_{80}\text{Zr}_{16}\text{B}_4$  ingot and of the samples melt spun with  $v_s = 48$  and 69 m/s. Whereas the ingot sample and the sample melt spun with  $v_s = 48$  m/s are crystalline, the sample melt spun with  $v_s = 69$  m/s is partially crystalline and partially amorphous. The lines present in the x-ray diffraction patterns of

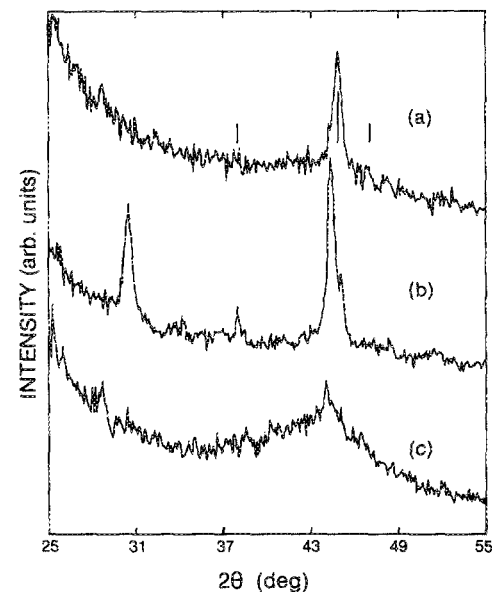


FIG. 3.  $\text{CuK}\alpha$  x-ray diffraction patterns for (a)  $\text{Co}_{80}\text{Zr}_{16}\text{B}_4$  ingot and samples melt spun from it at (b)  $v_s = 48$  m/s and (c)  $v_s = 69$  m/s. The vertical lines, whose length is proportional to their intensities, correspond to the three strongest lines of fcc  $\text{Co}_5\text{Zr}$  with  $a = 0.670$  nm.

$\text{Co}_{80}\text{Zr}_{16}\text{B}_4$  (Fig. 3) and of other compositions could not be assigned to possible standard crystalline phases such as  $\text{Co}_4\text{Zr}$ ,  $\text{Co}_{23}\text{Zr}_6$ ,  $\text{Co}_2\text{Zr}$ ,  $\text{CoZr}$ ,  $\text{CoZr}_2$ ,  $\text{CoZr}_4$ ,  $\alpha\text{-Co}$ ,  $\beta\text{-Co}$ , or to various Co-B alloys. This suggests that a new crystalline phase (or phases) is formed in the  $\text{Co}_{80}\text{Zr}_{20-x}\text{B}_x$  system. Such a new phase can be associated with fcc  $\text{Co}_5\text{Zr}$  isomorphous with  $\text{Ni}_5\text{Zr}$ . This new phase was also observed in the crystallization product of  $\text{Co}_{90}\text{Zr}_{10}$  and  $\text{Co}_{88}\text{Zr}_{12}$  glasses.<sup>7</sup> The three strongest lines of  $\text{Co}_5\text{Zr}$  calculated for  $a = 0.670$  nm match well with some of the experimental lines present in the x-ray diffraction patterns of  $\text{Co}_{80}\text{Zr}_{16}\text{B}_4$  (Fig. 3) and of other compositions studied here. It is possible that the magnetic properties of the  $\text{Co}_{80}\text{Zr}_{20-x}\text{B}_x$  series is determined by the presence of this new phase.

#### IV. CONCLUSION

The magnetic parameters of the  $\text{Co}_{80}\text{Zr}_{20-x}\text{B}_x$  alloys depend critically on the quench rate. The optimized values of  $H_c = 2.68$  kOe and  $(BH)_{\text{max}} = 2.10$  Mg Oe were obtained for  $\text{Co}_{80}\text{Zr}_{16}\text{B}_4$  melt-spun with  $v_s = 48$  m/s. The presence of a new crystalline phase  $\text{Co}_5\text{Zr}$  was found. The mag-

netic behavior of this system is probably associated with this phase.

#### ACKNOWLEDGMENTS

This work was supported by the Natural Science and Engineering Research Council of Canada. The technical assistance provided by Ben Fullerton is greatly appreciated.

<sup>1</sup>A. M. Ghemawat, M. E. McHenry, and R. C. O'Handley, *J. Appl. Phys.* **63**, 3388 (1988).

<sup>2</sup>A. M. Ghemawat, M. Foldeaki, R. A. Dunlap, and R. C. O'Handley, *IEEE Trans. Magn.* **25**, 3312 (1989).

<sup>3</sup>C. D. Fuerst and J. F. Herbst, *J. Appl. Phys.* **66**, 1782 (1989), and references therein.

<sup>4</sup>N. Heiman and N. Kazama, *Phys. Rev. B* **17**, 2215 (1978).

<sup>5</sup>C. D. Fuerst and J. F. Herbst, *J. Appl. Phys.* **64**, 1332 (1988).

<sup>6</sup>K. H. J. Buschow, in *Ferromagnetic Materials*, edited by E. P. Wohlfarth and K. H. J. Buschow (Elsevier, Amsterdam, 1988), Vol. 4, p. 1; K. J. Strnat, *ibid.*, p. 131.

<sup>7</sup>Z. Altounian, E. Batalla, and J. O. Strom-Olsen, *J. Appl. Phys.* **59**, 2364 (1986).